Ambient Backscatter: A New Approach to Improve Network Performance for RF-Powered Cognitive Radio Networks

Dinh Thai Hoang, Member, IEEE, Dusit Niyato, Fellow, IEEE, Ping Wang, Senior Member, IEEE, Dong In Kim, Senior Member, IEEE, and Zhu Han, Fellow, IEEE

Abstract—This paper introduces a new solution to improve the performance for secondary systems in radio frequency (RF) powered cognitive radio networks (CRNs). In a conventional RFpowered CRN, the secondary system works based on the harvestthen-transmit protocol. That is, the secondary transmitter (ST) harvests energy from primary signals and then uses the harvested energy to transmit data to its secondary receiver (SR). However, with this protocol, the performance of the secondary system is much dependent on the amount of harvested energy as well as the primary channel activity, e.g., idle and busy periods. Recently, ambient backscatter communication has been introduced, which enables the ST to transmit data to the SR by backscattering ambient signals. Therefore, it is potential to be adopted in the RF-powered CRN. We investigate the performance of RF-powered CRNs with ambient backscatter communication over two scenarios, i.e., overlay and underlay CRNs. For each scenario, we formulate and solve the optimization problem to maximize the overall transmission rate of the secondary system. Numerical results show that by incorporating such two techniques, the performance of the secondary system can be improved significantly compared with the case when the ST performs either harvest-then-transmit or ambient backscatter technique.

Index Terms—Cognitive radios, ambient backscatter, RF energy harvesting, convex optimization.

I. INTRODUCTION

OGNITIVE radio is an intelligent radio network which aims to utilize available spectrum that becomes more and more scarce due to the tremendous growth of wireless

Manuscript received October 19, 2016; revised March 2, 2017 and May 11, 2017; accepted May 22, 2017. Date of publication June 1, 2017; date of current version September 14, 2017. This work was supported by the National Research Foundation of Korea Grant Funded by the Korean Government (MSIP) under Grant 2014R1A5A1011478; Singapore MOE Tier 1 (RG33/16 and RG18/13) and MOE Tier 2 (MOE2014-T2-2-015 ARC4/15 and MOE2013-T2-2-070 ARC16/14); US NSF CNS-1702850, CNS-1646607, ECCS-1547201, CCF-1456921, CMMI-1434789, CNS-1443917, and ECCS-1405121. This paper was presented at the IEEE GLOBECOM 2016 [1]. The associate editor coordinating the review of this paper and approving it for publication was W. Zhang. (Corresponding author: Dong In Kim.)

- D. T. Hoang, D. Niyato, and P. Wang are with Nanyang Technological University, Singapore 639798 (e-mail: dinh0007@e.ntu.edu.sg; dniyato@ntu.edu.sg; wangping@ntu.edu.sg).
- D. I. Kim is with Sungkyunkwan University, Seoul 440-746, South Korea (e-mail: dikim@skku.ac.kr).
- Z. Han is with the University of Houston, Houston, TX 77004 USA (e-mail: zhan2@uh.edu).

Color versions of one or more of the figures in this paper are available online at http://ieeexplore.ieee.org.

Digital Object Identifier 10.1109/TCOMM.2017.2710338

communication demand. Recently, with the development of radio frequency (RF) energy harvesting techniques, a new type of networks has been introduced, i.e., an RF-powered cognitive radio network (CRN) [2]–[5]. In this network, the secondary transmitter (ST) is able to harvest energy from primary signals, and then uses the harvested energy to transmit data to its secondary receiver (SR) through a primary channel without causing harmful interference to primary users. The transmission used in the current RF-powered CRNs is therefore known as the harvest-then-transmit protocol/mode [3], [5]. However, the performance of RF-powered CRNs depends largely on the amount of harvested energy and the primary channel activity. For example, when the amount of harvested energy is too small and/or the channel idle period of the overlay CRNs is too short, the total transmitted bits will be remarkably reduced. Therefore, we need to find alternative solutions to overcome this limitation and achieve the best performance for the secondary system.

Ambient backscatter communication [6]–[8] recently has been introduced, which enables wireless nodes to communicate through using ambient signals without requiring any form of active radio transmission. In ambient backscatter communication, when a transmitter wants to send data to its receiver, the transmitter backscatters ambient signals, e.g., TV or WiFi signals, to its receiver. The receiver can decode and obtain the data by using averaging mechanisms [6]. However, the performance of ambient backscatter communication depends on the availability of primary signals. Therefore, in this paper, we introduce a novel concept of integrating ambient backscatter communication into RF-powered CRNs with the aim of improving the performance of the secondary system in terms of the overall data transmission rate.

In particular, we present an RF-powered backscatter CRN which enables the ST not only to harvest energy from primary signals, but also to backscatter these signals to the SR for data transmission. Nevertheless, as stated in [9], ambient backscatter communication and RF energy harvesting processes cannot be efficiently performed at the same time in practice. If the ST backscatters signals, the RF carrier will be modulated by reflection, causing significant reduction in the harvested energy, and mostly the energy is insufficient for data transmission. Consequently, this leads to a question of how to choose the best mode, i.e., the harvest-then-transmit mode or backscatter mode, given the current radio conditions

such that the total transmitted bits received at the SR per time unit is maximized. As such, we formulate and solve optimization problems to find an optimal transmission policy for the ST. Moreover, we analyze and evaluate the performance of the secondary system under different scenarios. Through the numerical results, we demonstrate that by integrating ambient backscatter communication into the RF-powered CRN, the performance of the secondary system can be significantly enhanced. Additionally, we reveal some insights which can be used as a benchmark for implementing such two transmission techniques (i.e., harvest-then-transmit and ambient backscatter) for secondary systems.

The paper is organized as follows. In Section II, we present the related work and highlight the main contributions of this paper. Then, in Section III and Section IV, we study two scenarios in CRNs, i.e., overlay and underlay CRNs, respectively. Next, experiments are performed to evaluate the efficiency of the proposed solutions in Section V. The conclusion together with future work are presented in Section VI.

II. RELATED WORK AND MAIN CONTRIBUTIONS

A. Related Work

- 1) RF-Powered Cognitive Radio Networks: RF energy harvesting is a technique which enables a wireless node to convert electromagnetic energy from received radio waves into useful electric energy. Although RF energy harvesting is new, it has been receiving a lot of attentions especially in cognitive radio networks (CRNs) due to its outstanding advantages [10]. As a result, there are many research works focusing on finding the optimal solutions to improve the performance of RF-powered CRNs. The related work can be classified into four main topics as follows.
- a) Channel access: In [2], the authors introduced a channel access strategy for a secondary transmitter (ST) with the aim of maximizing its throughput through using a Markov chain and stochastic geometry model. In the system under consideration, the ST harvests energy if it is close enough to the primary transmitters, whereas it transmits data to the destination if it is sufficiently far from the primary receivers. Different from [2], the authors in [11] presented an idea for an ST to access the primary channel in an overlay CRN. In particular, the ST will harvest energy if the primary channel is busy, and transmit data if this channel is idle.
- b) Channel selection: While in [11], the authors just considered one primary channel at a time, the authors in [13] studied a more general case with multiple primary channels that the secondary system can utilize at the same time. Different channels have different capacities, e.g., high or low channel idle probabilities. Thus, the ST needs to choose the best channel to access at each time slot such that its average throughput is maximized. For example, in the case that the ST wants to transmit data, it will select the channel with a high idle probability. By contrast, if the ST wants to harvest energy, it will prefer the channel with a low idle probability. This work then was extended to the case with multiple secondary users in [10].

- c) Relaying: In [12], the authors studied an application of the RF energy harvesting technique for a secondary relaying network. Specifically, when the primary channel is idle, the ST will transmit data to its secondary relay node. When the relay node receives the signal, it will extract the useful information and at the same time harvest energy from the received signal. Then, the relay node will use the harvested energy to forward data to the secondary receiver (SR). Extended from [12], the authors in [14] designed an RF-powered cognitive relay network to relay data of primary systems. The ST harvests energy from the received primary signals and then forwards such primary signals together with its own signals to the corresponding destinations.
- d) Time scheduling: In [15], the authors proposed an online solution to find an optimal trade-off time between the energy harvesting phase (EHP) and the data transmission phase (DTP) for an underlay CRN. In the EHP, the ST harvests energy from the PT's signals and uses this energy to transmit data in the DTP under interference constraints of the primary system. Then, to determine the optimal trade-off time between the EHP and DTP, the authors adopted the convex optimization technique and derived the optimal value for the time-sharing ratio. A similar scenario was also examined in [16], but the authors in [16] considered a cooperation between the primary system and the secondary system. Specifically, in the second phase, the ST can opt to transmit data to its destination or relay data for the primary system. Consequently, the ST has to determine not only how much time on the EHP, but also how much power for data relay or data transmission.
- 2) Ambient **Backscatter** Communication: Ambient backscatter communication is a technique which allows two wireless nodes to communicate without a need of active radio transmission components [6], [7]. For example, we consider a secondary system with a secondary transmitter (ST) and a secondary receiver (SR) in the communication area of a primary system (e.g., the broadcast area of a TV towel), and the ST wants to send a packet to the SR. In this case, instead of initiating a transmission in the idle period of the TV channel, the ST can backscatter the TV signals to convey bits in the packet to the SR in the busy period of the TV channel. In particular, the ST can indicate bit '1' or bit '0' by switching its antenna between reflecting or non-reflecting state, respectively. Accordingly, when the SR receives reflected signals from the ST, it can decode as bits '1', and '0' otherwise.

The idea of using ambient backscatter techniques has quickly received great attentions from research communities because it is expected to "bring us closer to an Internet-of-Things" [17]. Recent research work has been focusing on improving the performance for ambient backscatter communication. Specifically, in [7], the authors extended [6] by employing multiple antennas and a novel coding mechanism to improve the backscatter transmission rate as well as the communication range. Through experiments, it was shown in [7] that the backscatter transmission rate and the backscatter communication range can be extended up to 1 Mbps and 20 meters, respectively. In [7], Parks et al. developed a coding scheme based on the spread spectrum techniques in

which each data bit is represented by one symbol, and each symbol in turn is represented by a predefined chip sequence. Different from [7], the authors in [18] proposed a new coding scheme which encodes several bits in a single symbol with the aim of increasing the data rate for ambient backscatter communication. Additionally, there are some other works which considered the security problem [19], and signal detection together with BER analysis [20] for ambient backscatter communication systems.

The development of ambient backscatter techniques is particularly appropriate to implement in RF-powered CRNs because of many reasons. First, similar to the RF-powered CRNs, ambient backscatter techniques also utilize ambient signals, e.g., TV signals, to allow secondary nodes to communicate. Second, with ambient backscatter techniques, secondary users can communicate without requiring decoding primary signals, which is particularly suitable to CRNs where secondary systems are unable and/or not allowed to decode primary signals. Third, integrating ambient backscatter techniques into RF-powered wireless nodes is convenient and simple. Ambient backscatter circuits are designed to be small in size, which are ultra-low-power devices [6], and thus they can be integrated into RF-powered wireless nodes efficiently.

B. Novelty, Applications, and Main Contributions

From all above work and others in the literature, to the best of our knowledge, there is no work considering an integration of ambient backscatter communication with RF-powered CRNs. In fact, ambient backscatter communication can be implemented easily and conveniently on wireless nodes because it just requires a circuit with simple components [6], [7]. In our design, an energy harvesting circuit and/or an ambient backscatter circuit will be integrated into a sensor to harvest energy and backscatter signals for the sensor, respectively. In practice, energy harvesting and ambient backscatter circuits are tiny and consume a small amount of energy which are suitable for sensors. For example, RFD102A (RF-DC Converter) module has the size of only 5mm × $7 \text{mm} \times 1.8 \text{mm}$, and its energy harvesting efficiency can reach up to 50% [21]. Furthermore, ADG902 RF switch [22] used in ambient backscatter circuit is even smaller than RFD102A, and its energy consumption for backscatter mode is very small with only $0.25 \mu W$. Thus, they are particularly suitable for the sensor. Moreover, the integration can significantly enhance the communication efficiency for secondary systems. Through numerical results, we will demonstrate that by integrating ambient backscatter technique, the total transmitted bits of the secondary system can be improved remarkably even under different environment conditions as well as hardware configurations. Thus, this paper is dedicated to analyzing the performance of the RF-powered CRNs with ambient backscatter communications.

As pointed out in [7], the communication range of the ambient backscatter technique can be achieved up to 20 meters. Therefore, this technique is especially appropriate to implement in sensor systems where sensor nodes are hardware-constrained devices, and communicate with the gateway in a short communication area. In particular, RF-powered backscatter CRNs can be implemented in sensor systems such as in smart houses, offices, hospitals, and so on. Depending on nearby ambient signals, e.g., WiFi signals or TV signals, sensors can choose backscatter mode, harvest-then-transmit mode, or hybrid mode (i.e., trade-off between backscatter and harvest-then-transmit modes) to maximize efficiency in transmitting information to the gateway.

The main contribution of this paper is threefold. First, we investigate the performance and present the overall transmission rate optimization problem for the secondary system in an RF-powered overlay CRN with ambient backscatter communication. Second, we optimize the performance of the secondary system in an RF-powered backscatter underlay CRN. Third, we perform extensive performance evaluation with the aim of not only demonstrating the efficiency of the proposed solution, but also providing insightful guidance on the implementation of secondary systems.

III. RF-POWERED BACKSCATTER OVERLAY COGNITIVE RADIO NETWORK

A. Network Model

We study an RF-powered backscatter overlay cognitive radio network³ (CRN) composed of a primary system and a secondary system. In the secondary system, the secondary transmitter (ST) communicates with a secondary receiver (SR) via the primary channel. The ST is equipped with an RF energy harvesting circuit and a backscatter circuit to harvest RF energy and backscatter radio signals, respectively. The ST can also transmit data as normal wireless transmission. When the PT, e.g., a frequency modulated (FM) broadcasting base station (BS) or a TV tower, transmits RF signals to its primary receiver (PR), the primary channel is busy. It is assumed that in the busy period, signals received at the secondary system are continuous and stable. Let us take Disney TV channel in Singapore [23] as an example. This channel broadcasts programs continuously daily from 5 AM to 11 PM and ceases at night. Thus, in the busy period, the ST can either harvest energy and store it in an energy storage or backscatter the signal for data transmission. The harvested energy is used for direct wireless data transmission to the SR when the primary channel becomes idle. This is referred to as the harvest-thentransmit mode while the other is referred to as the backscatter mode.

In the proposed system, when the PT transmits signals, the ST can transmit data to the SR using backscatter communication (Fig. 1(a)) or harvest energy (Fig. 1(b)). Let β denote the normalized channel idle period, and $(1 - \beta)$ denote the normalized channel busy period as shown in Fig. 1. For example, in the case of Disney TV channel in Singapore [23]

¹For RF-powered CRNs, the ST harvests energy from TV signals, and then uses this energy to transmit data to the SR.

²A basic block diagram of an ambient backscatter device which allows a wireless node to either harvest energy or backscatter primary signals can be found in [6].

³In overlay CRNs, a secondary user is allowed to transmit signals to a primary channel iff this channel is currently not occupied by primary users.

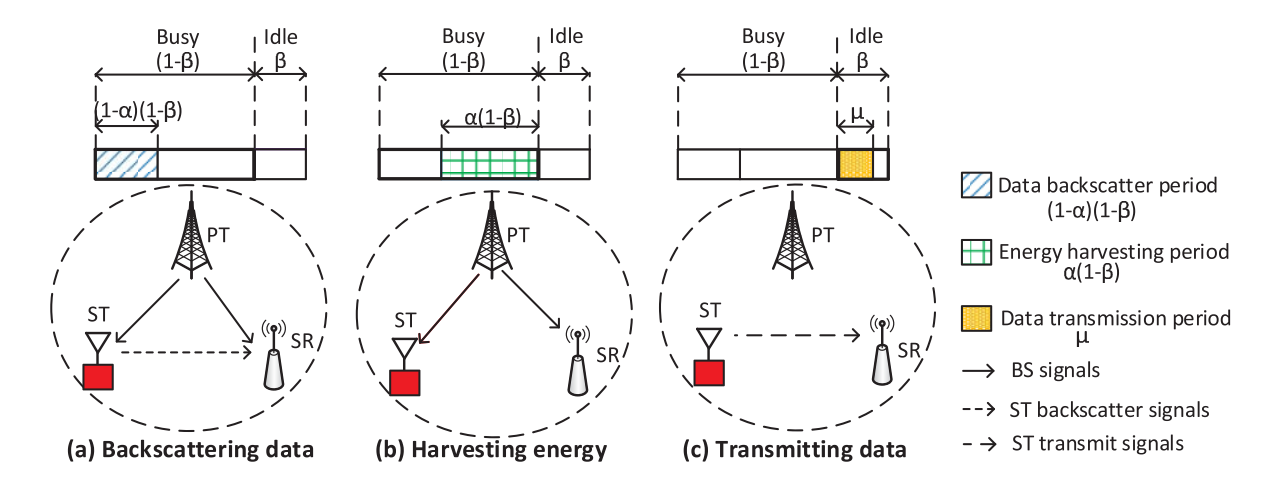


Fig. 1. RF-powered overlay cognitive radio network with ambient backscatter communication.

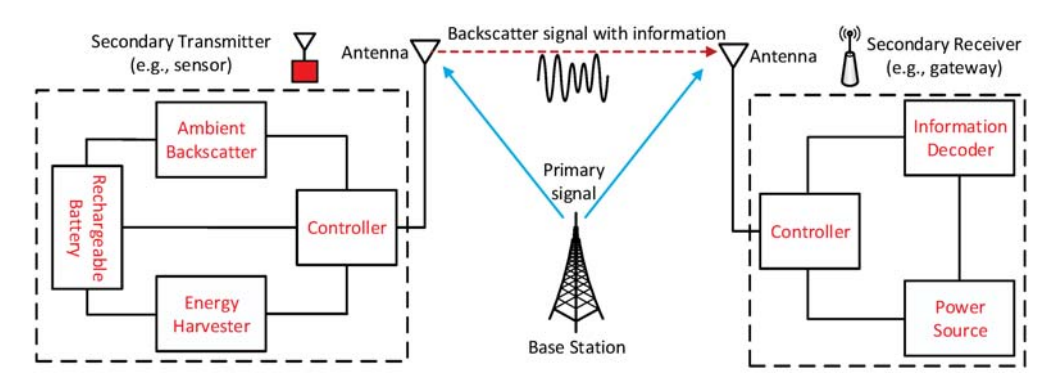


Fig. 2. Circuit diagram for the RF-powered backscatter CRNs.

which broadcasts programs continuously daily from 5 AM to 11 PM and ceases at night, the normalized time frame is a day (i.e., 24 hours), and thus the normalized channel idle period will be approximately 0.25 (i.e., 25%). It is also noted that for overlay CRNs, as long as signals are continuously emitted from the PT during the busy period, the SR can decode information received from the ST successfully by the ambient backscatter technique [6].

When the channel is busy, α denotes the time fraction for energy harvesting, and thus $(1-\alpha)$ denotes the time fraction for backscatter communication. The energy harvested during the time fraction α will be stored in the ST's energy storage before it is used for direct data transmission during the channel idle period (Fig. 1(c)). We observe that there is a tradeoff between the time fractions for backscatter communication and energy harvesting. Clearly, the ST can achieve an optimal overall transmission rate through the dual mode of harvest-then-transmit and backscatter by balancing between backscatter communication and energy harvesting time during the channel busy period. Thus, in Section III-C, we will formulate and solve the optimization problem to find an optimal value of α for the ST.

B. Circuit Diagram

Fig. 2 shows conceptually a circuit diagram implemented at the secondary transmitter (ST) and the secondary receiver (SR). The ST, e.g., a wireless sensor, consists of four

main components, i.e., a controller, an ambient backscatter, an energy harvester, and a rechargeable battery. The controller is responsible for selecting the operating mode, i.e., ambient backscatter or energy harvesting, and proceeds accordingly. When the primary channel is busy, if the ST chooses the energy harvesting mode, it will harvest energy from primary signals and store in the battery which will be used to transmit data to the SR when the channel becomes idle. Otherwise, if the ST chooses the backscatter mode, it will backscatter signals to the SR with information. It is noted that in the backscatter mode, the ST still can harvest energy, but the amount of harvested energy is relatively small and just sufficient to supply for operations in the backscatter mode.

Similar to the ST, SR (e.g., a gateway) is also equipped with a controller and a power source. However, since the gateway is often a fixed node, the SR's power source is much more stable and powerful than that of the ST. Moreover, the SR uses a decoder circuit to decode information received from the ST. The decoder circuit is used to decode information when the ST backscatters signals in the busy period or when the ST transmits signals in the idle period. The detail of the decoder circuit is provided in [6]. Note that to expand the communication range between the ST and the SR, the coding mechanism implemented in [7] can be adopted.

It is important to note that RF-powered backscatter CRNs are particularly suitable to implement in sensor systems because of the following reasons. On the one hand, ambient

backscatter circuits are lightweight with low-power consumption, and thus they are convenient to integrate into hardware-constrained devices, e.g., sensors. On the other hand, decoder circuits which often require more energy consumption with complex design, can be implemented on the gateway which is often equipped with more powerful hardware.

C. Problem Formulation

We aim at maximizing the overall transmission rate of the secondary system, which is the number of information bits transmitted by the ST per time unit. We denote R as the overall transmission rate which is obtained from

$$R = R_{\rm b} + R_{\rm h},\tag{1}$$

where R_b and R_h are the numbers of transmitted bits using the backscatter mode and the harvest-then-transmit mode in a time unit, respectively. Here, we note that in the case of the backscatter mode, we do not need to consider the interference to the primary receiver because through real experiments in [6] it was demonstrated that the backscattering transmitter does not create any noticeable glitches at the primary receiver unless it is less than 7 inches.

1) Backscatter Mode: There were some research works in the literature studying and deriving the closed form of the ambient backscatter throughput, such as [24]–[26]. To derive the closed form of backscatter throughput for an ambient backscatter system, the receiver needs to be able to sample the received signals to demodulate and decode information. However, acquiring digital samples requires an analog-to-digital converter (ADC) which can consume a significant amount of power and is typically avoided in ultra-low-power designs [27]. Therefore, in this paper, we follow the decoding mechanism proposed in [6] for ultra-low power systems, which is especially relevant to our considered system model.

Under the proposed mechanism in [6], the receiver can decode information with a high energy efficiency. Nevertheless, in this case, we are unable to derive the closed form of the backscatter throughput for the ambient backscatter mode because now the backscatter throughput will depend particularly on the decoding circuit. Thus, the achievable backscatter rate of a given ambient backscatter system only can be measured through real experiments. In the paper, we assume that the achievable backscatter rate of the ambient backscatter system can be obtained in advance through real testing experiments. Then, the total number of bits transmitted using the backscatter mode per time unit for the RF-powered backscatter CRN is expressed as follows:

$$R_{\rm b} = (1 - \beta)(1 - \alpha)B_{\rm b},$$
 (2)

where B_b represents the achievable backscatter rate of the backscatter mode, i.e., the number of bits decoded successfully at the receiver. Here, we note that based on real implementations in [6], when the ST backscatters signals to the SR, the ST can still harvest energy from RF signals (e.g., when RF signals are absorbed for bit '0'). Although the amount of harvested energy is not enough to transmit data when the channel is idle, it is sufficient to sustain backscatter operations

of the ST. Therefore, in (2), there is no need to consider the circuit energy consumption for the backscatter mode.

- 2) Harvest-Then-Transmit Mode: The harvest-then-transmit mode includes two phases. First, the ST harvests energy from the PT signals when the channel is busy. Then, the ST uses the harvested energy to transmit data when the primary channel becomes idle.
- a) Harvesting energy: In this paper, we adopt the free space model which is commonly used in wireless energy harvesting in the literature. Furthermore, in the numerical results, we will evaluate impacts of different signals, e.g., TV and WiFi signals, as well as the distance from the PT to the secondary system, to the ST's decisions (e.g., based on the amount of harvested energy). Thus, the free space model is appropriate for analysis purpose in this paper. However, note that the proposed framework can be applied to any energy harvesting models.

From the Friis equation [28], we can determine the harvested RF power from the PT signals at the ST in a free space as follows:

$$P_{\rm R} = \delta P_{\rm T} \frac{G_{\rm T} G_{\rm R} \lambda^2}{(4\pi d)^2},\tag{3}$$

where P_R is the harvested power of the ST, P_T is the PT transmit power, $\delta \in [0, 1]$ is the energy harvesting efficiency, G_T is the PT antenna gain, G_R is the ST antenna gain, λ is the emitted wavelength, and d is the distance between the PT and ST. We then derive the total amount of harvested energy over the energy harvesting period $\alpha(1 - \beta)$ as follows:

$$E_{\rm h} = \alpha (1 - \beta) P_{\rm R} = \alpha (1 - \beta) \delta P_{\rm T} \frac{G_{\rm T} G_{\rm R} \lambda^2}{(4\pi d)^2}.$$
 (4)

b) Transmitting data: In the harvest-then-transmit mode, after harvesting energy, the ST uses all harvested energy deducted by the circuit energy consumption to transmit data over the data transmission period μ when the channel is idle. Let $P^{\rm tr}$ denote the transmit power of the ST in the data transmission period μ ($\mu \in [0, \beta]$ as shown in Fig. 1(c)) when the channel is idle. Then, $P^{\rm tr}$ can be obtained from

$$P^{\rm tr} = \frac{E_{\rm h} - E_{\rm c}}{\mu},\tag{5}$$

where E_h is the total harvested energy and E_c is the circuit energy consumption in the transmission time μ . From [29], given the transmit power P^{tr} , the transmit data rate can be determined as follows:

$$r_{\rm h} = \kappa W \log_2 \left(1 + \frac{P^{\rm tr}}{P_0} \right),\tag{6}$$

where $\kappa \in [0, 1]$ is the data transmission efficiency, W is the bandwidth of the primary channel, and P_0 is the ratio between the noise power N_0 and the channel gain coefficient h, i.e., $P_0 = \frac{N_0}{h}$.

Then, the number of transmitted bits per time unit using the harvest-then-transmit mode is given by

$$R_{\rm h} = \mu \kappa W \log_2 \left(1 + \frac{P^{\rm tr}}{P_0} \right) = \mu \kappa W \log_2 \left(1 + \frac{E_{\rm h} - E_{\rm c}}{\mu P_0} \right). \tag{7}$$

Here, since R_h in (7) must be non-negative, P^{tr} in (5) must be also non-negative. Therefore, from (5), we have the following constraint

$$E_{\rm h} = \alpha (1 - \beta) P_{\rm R} \ge E_{\rm c}$$
, it means (8)

$$\alpha \ge \frac{E_{\rm c}}{(1-\beta)P_{\rm R}}.\tag{9}$$

We denote $\alpha^\dagger=\frac{E_{\rm c}}{(1-\beta)P_{\rm R}}$ as the minimum energy harvesting time to obtain enough energy for supplying the circuit of the ST to use the harvest-then-transmit mode. Then, we have $\alpha \geq \alpha^{\dagger}$. Note that we have $\alpha \leq 1$. Therefore, if $\alpha^{\dagger} \leq 1$, then R_h can be greater than zero. We denote $m = \frac{(1-\beta)}{P_0\mu}P_R$ and $n = 1 - \frac{E_c}{P_0 u}$. Then, from (7), we have

$$R_{\rm h} = \begin{cases} \mu \kappa W \log_2(n + m\alpha), & \text{if } \alpha^{\dagger} \le 1 \text{ and } \alpha^{\dagger} \le \alpha, \\ 0, & \text{otherwise.} \end{cases}$$
 (10)

Here, we have m > 0 and $(n + m\alpha) \ge 1$, $\forall \alpha \in [\alpha^{\dagger}, 1]$.

Then, the overall transmission rate of the secondary system can be defined as (11), as shown at the bottom of this page.

In the next section, we will derive optimal values of α and μ such that the overall transmission rate of the secondary system is maximized.

D. Proposed Solution

First, from (11), when $R(\alpha, \mu) = (1 - \beta)(1 - \alpha)B_b$, it is easy to show that

$$\max_{\alpha,\mu} R(\alpha,\mu) = R(\alpha = 0) = (1 - \beta)B_b, \quad \forall \alpha \in [0,1].$$
 (12)

This implies that the ST will use only the backscatter mode when the primary channel is busy in this case.

Second, through Theorem 1, we will prove that when $\alpha^{\dagger} \leq 1$ and $\alpha^{\dagger} \leq \alpha$, an optimal overall transmission rate is achieved when the ST transmits data over the entire channel idle period, i.e., $\max_{\alpha,\mu} R(\alpha,\mu) = R(\alpha,\beta)$.

Theorem 1: When $\alpha^{\dagger} \leq 1$ and $\alpha^{\dagger} \leq \alpha$, if we consider R_h from (10) as a function of μ , then R_h reaches the highest value if and only if $\mu = \beta$. In other words,

$$\max_{\mu} R_{h}(\mu) = R_{h}(\beta), \quad \forall \mu \in [0, \beta]. \tag{13}$$

The proof of Theorem 1 is given in Appendix A.

From Theorem 1, the optimization problem in (11) can be rewritten with only one variable α as (14), as shown at the bottom of this page. Then, we give the following theorem.

Theorem 2: When $\alpha \in [\alpha^{\dagger}, 1]$ and $\alpha^{\dagger} < 1$ and the backscatter transmission rate

$$B_{\rm b} \in \left(\frac{\beta \kappa W m}{(m+n)(1-\beta)\ln 2}, \frac{\beta \kappa W m}{(ma^{\dagger}+n)(1-\beta)\ln 2}\right)$$
, there exists a globally optimal solution of $\alpha^* \in [\alpha^{\dagger}, 1]$ which maximizes R .

The proof of Theorem 2 is given in Appendix B.

The next theorem shows that if the backscatter transmission rate is high, the ST will backscatter as much as possible. Conversely, if the backscatter transmission rate is low, the ST will harvest energy for data transmission as much as possible.

Theorem 3: For
$$\alpha \in [\alpha^{\dagger}, 1]$$
 and $\alpha^{\dagger} \leq 1$, if $B_b \geq \frac{\beta \kappa W m}{(m\alpha^{\dagger} + n)(1 - \beta) \ln 2}$, then $\alpha^* = \alpha^{\dagger}$. Moreover, when $B_b \leq \frac{\beta \kappa W m}{(m+n)(1-\beta) \ln 2}$, then $\alpha^* = 1$.

The proof of Theorem 3 is given in Appendix C.

Finally, we can derive the maximum value of R as (15), as shown at the bottom of this page.

Here, we note that when $\alpha < \alpha^{\dagger}$, i.e., the amount of harvested energy in the busy period is not enough to supply for the ST's circuits for transmitting data in the idle period, the ST will choose the backscatter mode as shown in Fig. 6(a).

IV. RF-POWERED BACKSCATTER UNDERLAY COGNITIVE Radio Network

A. Network Model

Unlike "overlay" CRNs where the secondary transmitter (ST) can harvest RF energy when the primary channel is busy and transmit data when the channel is idle, in the "underlay" CRN, the primary channel is assumed to be always busy. Therefore, the ST has to control the transmit power in order to avoid causing harmful interference to the primary receiver (PR). Different from the RF-powered backscatter "overlay" CRN studied in Section III, in the RF-powered backscatter "underlay" CRN, we aim to determine an optimal trade-off among backscattering time, energy harvesting time, and transmitting time such that the overall transmission rate is maximized. Moreover, the interference to the primary system must be guaranteed under a predefined threshold. Note that the transmit power of the secondary system can be expressed as a function of the transmission time. This is because the transmit power can be calculated from the harvested energy and the total transmission time. Hence, in the following, we present an optimization problem considering the transmission time of the ST as a decision variable instead of the transmit power.

$$R(\alpha, \mu) = R_{\rm b} + R_{\rm h} = \begin{cases} (1 - \beta)(1 - \alpha)B_{\rm b} + \mu\kappa W \log_2(n + m\alpha), & \text{if } \alpha^{\dagger} \leq 1 \text{ and } \alpha^{\dagger} \leq \alpha, \\ (1 - \beta)(1 - \alpha)B_{\rm b}, & \text{otherwise.} \end{cases}$$
(11)

$$\max_{\alpha} R(\alpha) = \begin{cases}
(1 - \beta)(1 - \alpha)B_{b} + \beta\kappa W \log_{2}(n + m\alpha), & \text{if } \alpha^{\dagger} \leq 1 \text{ and } \alpha^{\dagger} \leq \alpha, \\
(1 - \beta)B_{b}, & \text{otherwise.}
\end{cases}$$

$$R_{\text{max}} = \begin{cases}
\max_{\alpha} \left[(1 - \beta)B_{b}, (1 - \beta)(1 - \alpha^{*})B_{b} + \beta\kappa W \log_{2}(n + m\alpha^{*}) \right], & \text{if } \alpha^{\dagger} \leq 1 \text{ and } \alpha^{\dagger} \leq \alpha, \\
(1 - \beta)B_{b}, & \text{otherwise.}
\end{cases}$$
(15)

$$R_{\text{max}} = \begin{cases} \max\left[(1 - \beta)B_{\text{b}}, (1 - \beta)(1 - \alpha^*)B_{\text{b}} + \beta\kappa W \log_2(n + m\alpha^*) \right], & \text{if } \alpha^{\dagger} \le 1 \text{ and } \alpha^{\dagger} \le \alpha, \\ (1 - \beta)B_{\text{b}}, & \text{otherwise.} \end{cases}$$
(15)

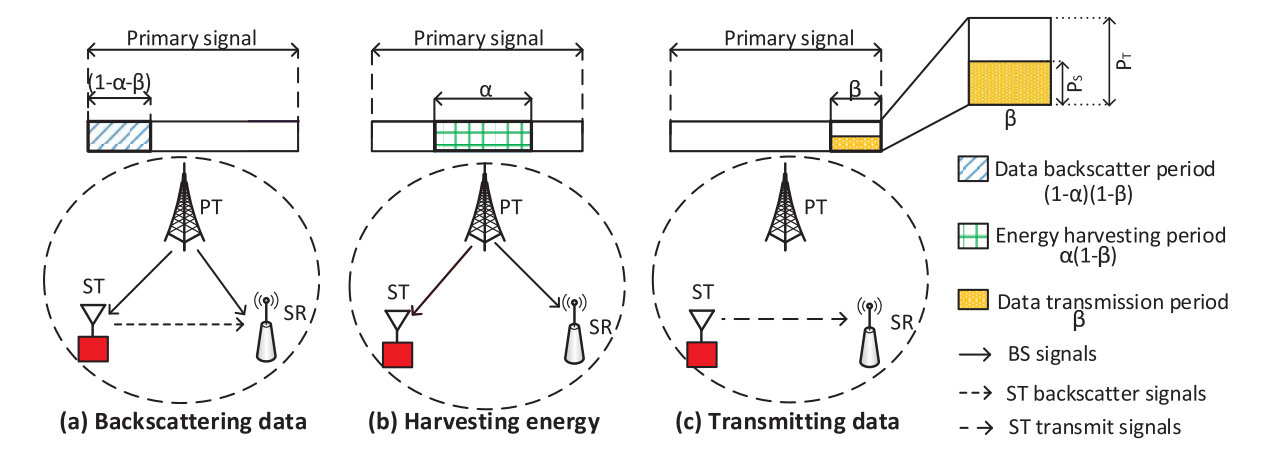


Fig. 3. RF-powered underlay cognitive radio network with ambient backscatter communication.

Similar to the case of the overlay CRN, we denote α as the time fraction for energy harvesting. However, the variable β now stands for the time fraction for data transmission instead of the channel idle period as in Section III. Consequently, the time fraction for backscattering will be $(1-\alpha-\beta)$ as illustrated in Fig. 3. Then, we have the following constraints, i.e., \mathbf{C}_0 , for the values of α and β .

$$\mathbf{C}_0 \quad \text{s.t.} \quad \begin{cases} \alpha, & \beta \ge 0, \\ \alpha + \beta \le 1. \end{cases}$$
 (16)

B. Problem Formulation

Again, we denote R, R_b and R_h as the total number of transmitted bits per time unit of the secondary system, from the backscatter mode, and from the harvest-then-transmit mode, respectively. For the case of the underlay CRN, we aim to maximize the overall transmission rate for the secondary system, i.e., R, under the transmit power constraint. We first formulate the optimization problem for the considered system, and then propose solutions to find the optimal trade-off for the ST by investigating the relation between the values of α and β .

1) Backscatter Mode: Similar to the previous section, the total number of bits transmitted by using the backscatter mode per time unit is determined as follows:

$$R_{\mathsf{h}} = (1 - \alpha - \beta)B_{\mathsf{h}},\tag{17}$$

where B_b is the transmission bit rate of the backscatter mode. 2) Harvest-Then-Transmit Mode:

a) Harvesting energy: Similar to the previous section, the total amount of harvested energy over the energy harvesting period is obtained as follows:

$$E_{\rm h} = \alpha P_{\rm R} = \alpha \delta P_{\rm T} \frac{G_{\rm T} G_{\rm R} \lambda^2}{(4\pi d)^2}.$$
 (18)

b) Transmitting data: After harvesting energy in the first phase, the ST uses all harvested energy deducted by the circuit energy consumption to transmit data over the data transmission period β . Let $P_{\rm S}$ denote the transmit power of the ST in the

data transmission period β . Thus, P_S can be obtained from

$$P_{\rm S} = \frac{E_{\rm h} - E_{\rm c}}{\beta},\tag{19}$$

where E_h is the total harvested energy, and E_c is the circuit energy consumption. If we denote P_c as the circuit power consumption of the ST, then $E_c = \beta P_c$. Note that we just consider the circuit energy consumption when the ST transmits data. When the ST harvests energy, the circuit energy consumption is negligible as discussed in [5], [11], [16], and [30].

For the considered underlay CRN, the transmit power of the ST must be lower than a predefined threshold to guarantee that the interference to the PR is acceptable. Thus, the following constraint is required

$$P_{\rm S} < P^{\ddagger}. \tag{20}$$

where P^{\ddagger} is the maximum transmit power allowed for the ST. For example, P^{\ddagger} can be set based on the carrier sensing threshold as presented in [31].

From (20), we derive the constraint for α and β as follows:

$$\frac{\alpha P_{\rm R} - E_{\rm c}}{\beta} \le P^{\ddagger}$$
, so
$$\alpha \le \beta \frac{P_{\rm c} + P^{\ddagger}}{P_{\rm R}}.$$
 (21)

From [29], given the transmit power P_S , the transmission rate can be obtained in a similar way as presented in (6) as follows:

$$r_{\rm h} = \kappa W \log_2 \left(1 + \frac{P_{\rm S}}{P_0} \right). \tag{22}$$

Then, the number of transmitted bits per time unit using the harvest-then-transmit mode is given by

$$R_{h} = \beta \kappa W \log_{2} \left(1 + \frac{P_{S}}{P_{0}} \right) = \beta \kappa W \log_{2} \left(1 + \frac{E_{h} - E_{c}}{\beta P_{0}} \right)$$
$$= \beta \kappa W \log_{2} \left(1 + \frac{\alpha P_{R} - \beta P_{c}}{\beta P_{0}} \right). \tag{23}$$

Here, since R_h in (23) must be non-negative, P_S in (19) must be also non-negative. Consequently, from (18) and (19), we have the following constraint

$$E_{\rm h} = \alpha P_{\rm R} \ge E_{\rm c}$$
, it means $\alpha \ge \frac{E_{\rm c}}{P_{\rm R}} = \frac{\beta P_{\rm c}}{P_{\rm R}}$. (24)

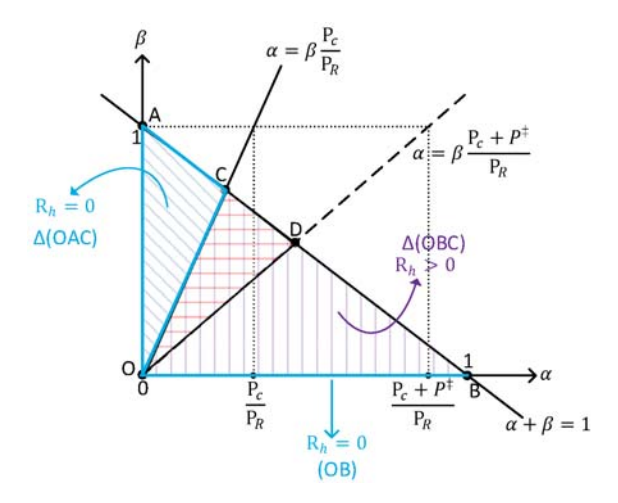


Fig. 4. Variable constraints.

The constraint in (24) implies that the length of the harvesting period must be sufficiently long to obtain energy and greater than the circuit energy consumption of the ST to use the harvest-then-transmit mode. Then, from (16), (20), (21), and (24), we derive the constraints for variables α and β as shown in Fig. 4.

In Fig. 4, the triangle (OAB) represents the feasible region of α and β which satisfies the constraint C_0 . The triangle (OAC) and the segment (OB) correspond to the case when $R_h = 0$, i.e., when the harvested energy is not enough to transmit data, i.e., $\alpha \leq \beta \frac{P_c}{P_R}$, and when the transmission period is zero, i.e., $\beta = 0$, respectively. The triangle (OBC) (not including the segments (OC) and (OB)) is the feasible region corresponding to the case when $R_h > 0$. The triangle (ODB)

(not including the segments (OB) and (OD)) corresponds to the case when $P_{\rm S} > P^{\ddagger}$. The triangle (ODC) excluding segment (OC) corresponds to the feasible region in which $R_{\rm h} > 0$ and the power constraint of the ST, i.e., $\alpha \leq \beta \frac{P_{\rm c} + P^{\ddagger}}{P_{\rm R}}$, is satisfied. Note that when $\alpha = 0$, i.e., there is no energy harvesting,

Note that when $\alpha = 0$, i.e., there is no energy harvesting, β must be zero. Likewise, when $\beta = 0$, i.e., the ST does not spend time for data transmission, then α must be zero because the harvested energy will not be used. Thus, from Fig. 4 and (23) we derive the formulation R_h as (25), as shown at the bottom of this page.

In (25), the constraint $\alpha \leq \beta \frac{P_{\rm c} + P^{\ddagger}}{P_{\rm R}}$ is applied when $R_{\rm h} > 0$ only. This is because when $R_{\rm h} = 0$ there is no interference to the primary system, and thus this constraint is not required. Then, the optimization problem can be formulated as (26), as shown at the bottom of this page.

In (26), it is easy to show that when $R(\alpha, \beta) = (1 - \alpha - \beta)B_b$, i.e., only the backscatter mode is used by the ST, the optimization problem is simplified to

$$\max_{\alpha,\beta} R(\alpha,\beta) = R(0,0) = B_{b}.$$
 (27)

Accordingly, the optimization problem in (26) can be written as (28), as shown at the bottom of this page.

C. Proposed Solution

We observe that α and β are not separate variables. For the harvest-then-transmit mode, they are dependent as indicated in [5] and [15]. Therefore, we first find the relation between α and β and then transform the optimization problem with two variables into a new optimization problem with only one variable, which is easier to solve and analyze.

$$R_{\rm h} = \begin{cases} \beta \kappa W \log_2 \left(1 + \frac{\alpha P_{\rm R} - \beta P_{\rm c}}{\beta P_0}\right), & \text{if } \alpha + \beta \leq 1, \alpha > 0, \beta > 0, \text{ and } \alpha > \beta \frac{P_{\rm c}}{P_{\rm R}}, \\ 0, & \text{if } \alpha + \beta \leq 1, \alpha > 0, \beta > 0, \text{ and } \alpha \leq \beta \frac{P_{\rm c}}{P_{\rm R}}, \text{ OR if } \alpha \beta = 0, \end{cases}$$
 s.t. $\alpha \leq \beta \frac{P_{\rm c} + P^{\ddagger}}{P_{\rm R}}.$ (25)

$$\max_{\alpha,\beta} R(\alpha,\beta) = \begin{cases} (1-\alpha-\beta)B_{\rm b} + \beta\kappa W \log_2 \left(1 + \frac{\alpha P_{\rm R} - \beta P_{\rm c}}{\beta P_{\rm 0}}\right), & \text{if } \alpha + \beta \leq 1, \alpha > 0, \beta > 0, \text{ and } \alpha > \beta \frac{P_{\rm c}}{P_{\rm R}}, \\ (1-\alpha-\beta)B_{\rm b}, & \text{if } \alpha + \beta \leq 1, \alpha > 0, \beta > 0, \text{ and } \alpha \leq \beta \frac{P_{\rm c}}{P_{\rm R}}, \\ \text{OR if } \alpha\beta = 0, & \text{s.t. } \alpha \leq \beta \frac{P_{\rm c} + P^{\ddagger}}{P_{\rm R}}. \end{cases}$$

$$(26)$$

$$\mathbf{P}_{1} \quad \max_{\alpha,\beta} R(\alpha,\beta) = \begin{cases} (1-\alpha-\beta)B_{\mathrm{b}} + \beta\kappa W \log_{2}\left(1 + \frac{\alpha P_{\mathrm{R}} - \beta P_{\mathrm{c}}}{\beta P_{0}}\right), & \text{if } \alpha + \beta \leq 1, \ \alpha > 0, \ \beta > 0, \ \text{and } \alpha > \beta \frac{P_{\mathrm{c}}}{P_{\mathrm{R}}}, \\ B_{\mathrm{b}}, & \text{if } \alpha + \beta \leq 1, \ \alpha > 0, \ \beta > 0, \ \text{and } \alpha \leq \beta \frac{P_{\mathrm{c}}}{P_{\mathrm{R}}}, \\ OR \text{ if } \alpha\beta = 0, \end{cases}$$

$$\mathbf{C}_{1} \quad \text{s.t. } \alpha \leq \beta \frac{P_{\mathrm{c}} + P^{\ddagger}}{P_{\mathrm{D}}}. \tag{28}$$

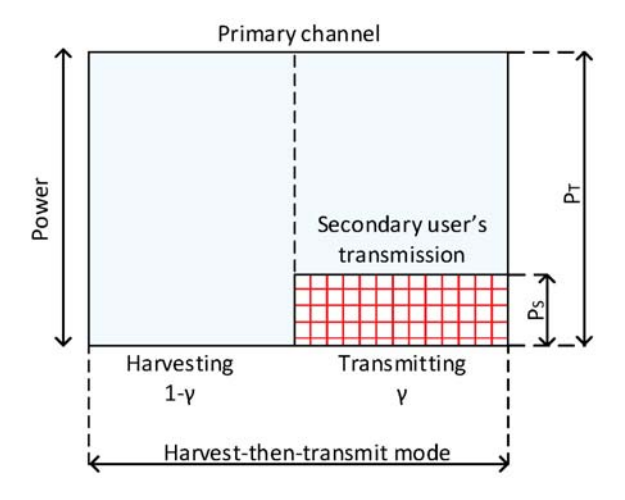


Fig. 5. Optimal time allocation for harvest-then-transmit mode.

1) Optimal Time Allocation for Harvest-Then-Transmit *Mode:* Here, we show that an optimal ratio between the energy harvesting period and the data transmission period can be found. Let γ denote the time fraction for the data transmission and $(1 - \gamma)$ denote the time fraction for the energy harvesting as shown in Fig. 5.

Similar to the previous section, we can derive the number of transmitted bits per time unit using the harvest-then-transmit mode as (29), as shown at the bottom of this page, by replacing $\alpha = (1 - \gamma)$ and $\beta = \gamma$ in (25).

The first condition $\alpha + \beta = (1 - \gamma) + \gamma \le 1$ is always satisfied. The second and third conditions

$$\alpha > 0$$
 and $\beta > 0$ are to ensure that $\gamma < 1$ and $\gamma > 0$, respectively. (30)

For the fourth condition in (29), we have

$$\alpha > \beta \frac{P_c}{P_R}$$
, so $1 - \gamma > \gamma \frac{P_c}{P_R}$. Thus $\gamma < \frac{P_R}{P_c + P_R}$. (31)

For the last condition in (29), we have

$$\alpha\beta = 0$$
, so $(1 - \gamma)\gamma = 0$, i.e., $\gamma = 0$ or $\gamma = 1$. (32)

From the constraint in (29), we have

$$\frac{\alpha P_{\rm R} \leq \beta P_{\rm c} + \beta P^{\ddagger},}{P_{\rm c} + P^{\ddagger} + P_{\rm R}} \leq \gamma. \tag{33}$$

Finally, from (30)-(33), we derive R_h as in (34), as shown at the bottom of this page.

Since $\frac{P_R}{P_c + P^{\ddagger} + P_R} < \frac{P_R}{P_c + P_R}$, for $\gamma \in (0, \frac{P_R}{P_c + P_R})$, the opti-

$$\mathbf{P}_{2} \quad \max_{\gamma} R_{h}(\gamma) = \gamma \kappa W \log_{2} \left(1 + \frac{(1 - \gamma) P_{R} - \gamma P_{c}}{\gamma P_{0}} \right),$$

C₂ s.t.
$$\begin{cases} \gamma < \frac{P_{R}}{P_{c} + P_{R}}, \\ \gamma \ge \frac{P_{R}}{P_{c} + P^{\ddagger} + P_{R}}. \end{cases}$$
 (35)

To simplify the presentation, we denote

$$a = \kappa W$$
, $b = 1 - \frac{P_{\rm R} + P_{\rm c}}{P_0}$, and $c = \frac{P_{\rm R}}{P_0}$. (36)

We can express the transmission rate of the harvest-thentransmit mode as follows:

$$R_{\rm h}(\gamma) = a\gamma \log_2\left(b + \frac{c}{\gamma}\right).$$
 (37)

From (37), we obtain the first derivative of R_h with respect to γ as follows:

$$R'_{h} = a \log_2 \left(b + \frac{c}{\gamma} \right) - \frac{ac}{(b\gamma + c) \ln 2}.$$
 (38)

In the following, we show that $R'_h = 0$ has a unique solution

Theorem 4: If $1 - \frac{P_R + P_c}{P_0} \ge (1 + \frac{P^{\ddagger}}{P_0}) (1 - \ln(1 + \frac{P^{\ddagger}}{P_0}))$, then we can always find a globally optimal solution γ_1^* for the optimization problem P_2 with the constraint C_2 that maximizes R_h .

The proof of Theorem 4 is provided in Appendix D. Theorem 5: If $1-\frac{P_R+P_c}{P_0}<(1+\frac{P^{\ddagger}}{P_0})(1-\ln(1+\frac{P^{\ddagger}}{P_0}))$, then we can always find a globally optimal solution γ_2^* for the optimization problem P_2 with constraint C_2 which maximizes R_h .

The proof of Theorem 5 is provided in Appendix E.

$$R_{\rm h} = \begin{cases} \gamma \kappa W \log_2 \left(1 + \frac{(1 - \gamma) P_{\rm R} - \gamma P_{\rm c}}{\gamma P_0} \right), & \text{if } \alpha + \beta \le 1, \ \alpha > 0, \ \beta > 0, \ \text{and } \alpha > \beta \frac{P_{\rm c}}{P_{\rm R}}, \\ 0, & \text{if } \alpha + \beta \le 1, \ \alpha > 0, \ \beta > 0, \ \text{and } \alpha \le \beta \frac{P_{\rm c}}{P_{\rm R}} \text{ OR if } \alpha \beta = 0, \end{cases}$$
 s.t. $\alpha \le \beta \frac{P_{\rm c} + P^{\ddagger}}{P_{\rm R}}.$ (29)

$$R_{h} = \begin{cases} \gamma \kappa W \log_{2} \left(1 + \frac{(1 - \gamma) P_{R} - \gamma P_{c}}{\gamma P_{0}} \right), & \text{if } \gamma \in (0, \frac{P_{R}}{P_{c} + P_{R}}), \\ 0, & \text{if } \gamma \in \left[\frac{P_{R}}{P_{c} + P_{R}}, 1 \right) \text{ OR if } (1 - \gamma) \gamma = 0, \end{cases}$$
s.t. $\gamma \geq \frac{P_{R}}{P_{c} + P^{\ddagger} + P_{R}}.$ (34)

From Theorem 4 and Theorem 5 we can derive optimal values of γ and R_h as in (39), as shown at the bottom of this page. where $\gamma_1^* = \frac{c}{X^* - b}$ and $\gamma_2^* = \frac{P_R}{P_c + P^* + P_R}$.

2) Optimal Time Tradeoff for Backscatter and Transmit-

Then-Harvest Mode: We denote

$$\gamma^* = \begin{cases} \gamma_1^*, & \text{if } 1 - \frac{P_R + P_c}{P_0} \ge (1 + \frac{P^{\ddagger}}{P_0}) \left(1 - \ln(1 + \frac{P^{\ddagger}}{P_0})\right), \\ \gamma_2^*, & \text{if } 1 - \frac{P_R + P_c}{P_0} < (1 + \frac{P^{\ddagger}}{P_0}) \left(1 - \ln(1 + \frac{P^{\ddagger}}{P_0})\right), \end{cases}$$

$$(40)$$

where $\gamma^* \in [\frac{P_R}{P_c + P^{\ddagger} + P_R}, \frac{P_R}{P_c + P_R})$. Also, let $\tau = \alpha + \beta$, we can derive that $\alpha = (1 - \gamma^*)\tau$ and $\beta = \tau \gamma^*$.

Now the optimization problem has been simplified to find an optimal time ratio, i.e., τ , between the backscatter mode and the harvest-then-transmit mode such that the overall transmission rate of the ST is maximized. Then, for $\tau \in [0, 1]$, we can rewrite the optimization problem P_1 as in (41), as shown at the bottom of this page.

For $\tau \in (0, 1]$, we observe that $R(\tau)$ is a linear function of

$$R'(\tau) = -B_b + \gamma^* \kappa W \log_2 \left(1 + \frac{(1 - \gamma^*) P_R - \gamma^* P_c}{\gamma^* P_0} \right), (44)$$

thus we derive the result as in (42), as shown at the bottom of this page.

Therefore, we have the result in (43), as shown at the bottom of this page.

In other words, the ST will select the backscatter mode if $B_b > \gamma^* \kappa W \log_2 \left(1 + \frac{(1-\gamma^*)P_R - \gamma^* P_c}{\gamma^* P_0}\right)$, and the harvest-then-transmit mode otherwise. Here, we note that when $B_b = \gamma^* \kappa W \log_2 \left(1 + \frac{(1-\gamma^*)P_R - \gamma^* P_c}{\gamma^* P_0}\right)$, then we have $R(\tau) = B_b = \gamma^* \kappa W \log_2 \left(1 + \frac{(1-\gamma^*)P_R - \gamma^* P_c}{\gamma^* P_0}\right)$. This implies that $R(\tau)$ is a constant. Therefore, the ST can choose either the backscatter mode or the harvest-then-transmit mode since both modes have the same transmission bit rate.

Let $B_{\rm b}^*=\gamma^*\kappa W\log_2\left(1+\frac{(1-\gamma^*)P_{\rm R}-\gamma^*P_{\rm c}}{\gamma^*P_0}\right)$ denote the threshold of the transmission rate of the backscatter mode, then the optimal transmission policy for the ST in this case can be simply expressed as a step function as follows:

ST's action =
$$\begin{cases} \text{Backscatter mode,} & \text{if } B_b \ge B_b^*, \\ \text{Harvest-then-transmit mode,} & \text{if } B_b < B_b^*. \end{cases}$$
(45)

V. NUMERICAL RESULTS AND PERFORMANCE EVALUATION

To evaluate the performance for the proposed solution, we show numerical results through performing simulation experiments for two scenarios, i.e., RF-powered "overlay" and "underlay" CRNs. For each scenario, we first show the overall transmission rate of the proposed solution with the primary signal being FM signal and examine the cases with other PTs, i.e., TV signal, 3G signal, and WiFi signal. Then, we investigate the transmission policy of the secondary transmitter (ST) under the variation of parameters and compare the performance of the proposed solution with other baseline policies, i.e., the harvest-then-transmit protocol [3], [5], and ambient backscatter communication [6], [7].

A. Experiment Setup

The parameters of the primary signals are provided in Table I. Here, we note that the transmit power from a macrocell base station (BS) and a small-cell access point (AP) is capped at 46 dBm and 24 dBm, respectively. Therefore, we set the transmit power of the cellular BS and WiFi AP at 10 dBm.

The other parameters are set as follows. The PT antenna gain and ST antenna gain are 6 dBi as in [32], and the circuit power consumption is -35 dBm. The energy harvesting efficiency and data transmission efficiency are 0.6. The channel idle period, the backscatter transmission rate, the transmit power constraint for the case of the underlay CRN, and the TV

$$(\gamma^*, R_h^*) = \begin{cases} (\gamma_1^*, R_h(\gamma_1^*)), & \text{if } 1 - \frac{P_R + P_c}{P_0} \ge (1 + \frac{P^{\ddagger}}{P_0}) (1 - \ln(1 + \frac{P^{\ddagger}}{P_0})), \\ (\gamma_2^*, R_h(\gamma_2^*)), & \text{if } 1 - \frac{P_R + P_c}{P_0} < (1 + \frac{P^{\ddagger}}{P_0}) (1 - \ln(1 + \frac{P^{\ddagger}}{P_0})), \end{cases}$$
(39)

$$\mathbf{P}_{3} \quad \max_{\tau} R(\tau) = \begin{cases} (1 - \tau)B_{b} + \tau \gamma^{*} \kappa W \log_{2} \left(1 + \frac{(1 - \gamma^{*})P_{R} - \gamma^{*} P_{c}}{\gamma^{*} P_{0}} \right), & \text{if } \tau \in (0, 1], \\ B_{b}, & \text{if } \tau = 0. \end{cases}$$
(41)

$$R(\tau) \begin{cases} \text{is a decreasing function,} & \text{if } R'(\tau) < 0, \text{ i.e., } B_{b} > \gamma * \kappa W \log_{2} \left(1 + \frac{(1 - \gamma *) P_{R} - \gamma * P_{c}}{\gamma * P_{0}} \right), \\ \text{is an increasing function,} & \text{if } R'(\tau) > 0, \text{ i.e., } B_{b} < \gamma * \kappa W \log_{2} \left(1 + \frac{(1 - \gamma *) P_{R} - \gamma * P_{c}}{\gamma * P_{0}} \right). \end{cases}$$

$$(42)$$

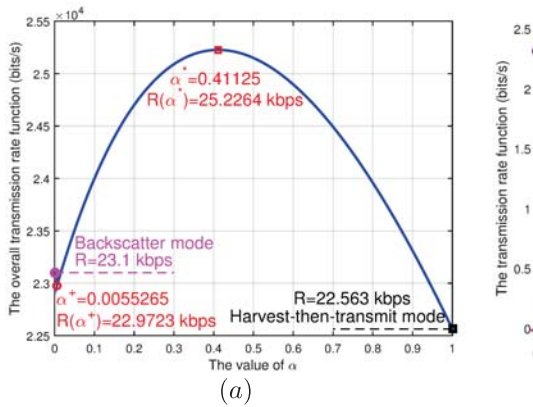
$$R(\tau) \begin{cases} \text{is a decreasing function,} & \text{if } R'(\tau) < 0, \text{ i.e., } B_{b} > \gamma * \kappa W \log_{2} \left(1 + \frac{(1 - \gamma^{*}) P_{R} - \gamma^{*} P_{c}}{\gamma^{*} P_{0}}\right), \\ \text{is an increasing function,} & \text{if } R'(\tau) > 0, \text{ i.e., } B_{b} < \gamma * \kappa W \log_{2} \left(1 + \frac{(1 - \gamma^{*}) P_{R} - \gamma^{*} P_{c}}{\gamma^{*} P_{0}}\right). \end{cases}$$

$$\max_{\tau} R(\tau) = \begin{cases} R(\tau = 0) = B_{b}, & \text{if } B_{b} > \gamma * \kappa W \log_{2} \left(1 + \frac{(1 - \gamma^{*}) P_{R} - \gamma^{*} P_{c}}{\gamma^{*} P_{0}}\right), \\ R(\tau = 1) = \gamma * \kappa W \log_{2} \left(1 + \frac{(1 - \gamma^{*}) P_{R} - \gamma^{*} P_{c}}{\gamma^{*} P_{0}}\right), & \text{if } B_{b} < \gamma * \kappa W \log_{2} \left(1 + \frac{(1 - \gamma^{*}) P_{R} - \gamma^{*} P_{c}}{\gamma^{*} P_{0}}\right). \end{cases}$$

$$(42)$$

TABLE I
REFERENCED PARAMETERS

RF source	Transmit power	Frequency	Bandwidth	Distance from the RF source to the secondary nodes
FM tower	17 kW	100 MHz	100 KHz	10782 meters (6.7 miles as in [6])
TV tower	17 kW	915 MHz	6 MHz	2000 meters
Cellular BS	10 dBm	2.15 GHz	14 MHz	100 meters
WiFi AP	10 dBm	2.4 GHz	20 MHz	2 meters



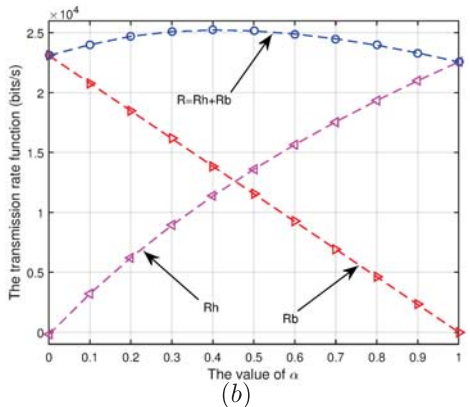
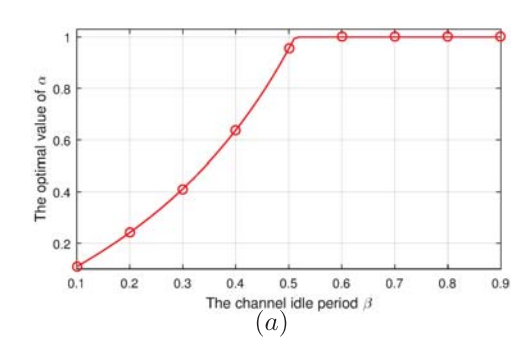


Fig. 6. The overall transmission rate under different values of α .



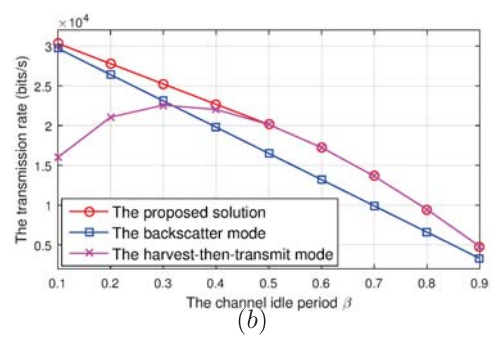


Fig. 7. The performance of the system under the variation of channel idle period.

signal frequency will be varied to evaluate the performance as well as the policy of the secondary system.

B. Overlay Cognitive Radio Networks

In Fig. 6(a), we first show the overall transmission rate $R(\alpha)$ in (14) as the value of α is varied. Here, we set the channel idle period at 0.3 (i.e., the RF source transmits signals continuously 70% of the total time) and the backscatter transmission rate at 33 kbps. In Fig. 6(a), we observe that if the ST uses either the backscatter mode or the harvest-thentransmit mode, then the overall transmission rates of the ST are 23.1 and 22.563 kbps, respectively. However, if the ST spends 41.125% of time (in the channel busy period) for the energy harvesting, i.e., $\alpha = 0.41125$, and 58.875% for backscattering, then the overall transmission rate of the secondary system can be up to 25.2264 kpbs. This can be explained through Fig. 6(b). As the value of α increases, R_b decreases linearly, while R_h increases following the logarithmic function. This is because when the value of α is too small, i.e., the ST spends much time for the backscattering, the ST cannot fully utilize the channel idle period for data transmission because of the small amount of harvested energy. Alternatively, if the value of α is too high, i.e., the ST spends much time for harvesting energy, the overall transmission rate will be low because the backscatter mode is not efficiently utilized during the channel busy period.

We vary the channel idle period β and observe its impact to the transmission policy as well as the performance of the secondary system. As shown in Fig. 7(a), when the channel idle period is increased from 0.1 to 0.5, the optimal value of α increases quickly from 0.1 to 0.95, and it then remains stable at 1 when β is greater than 0.5. Clearly, for the primary channel with low channel idle period, the ST will spend more time for the backscatter mode. By contrast, for the primary channel with a high channel idle period, the ST prefers the harvest-then-transmit mode. This is from the fact that the harvest-then-transmit mode can provide higher transmission rate than that of the backscatter mode. Hence, when the channel idle period is high, the ST will spend the whole time to harvest energy when the channel is busy.

In Fig. 7(b), we show the overall transmission rate obtained from the proposed solution and comparisons with two baseline

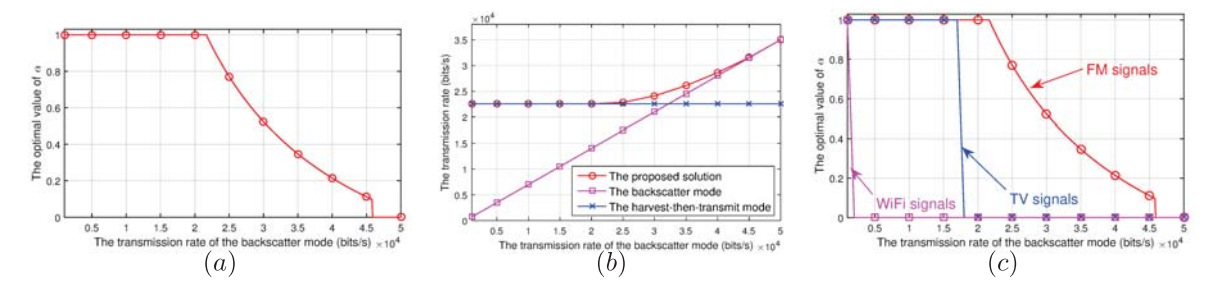


Fig. 8. The performance of the system under the variation of backscatter transmission rate.

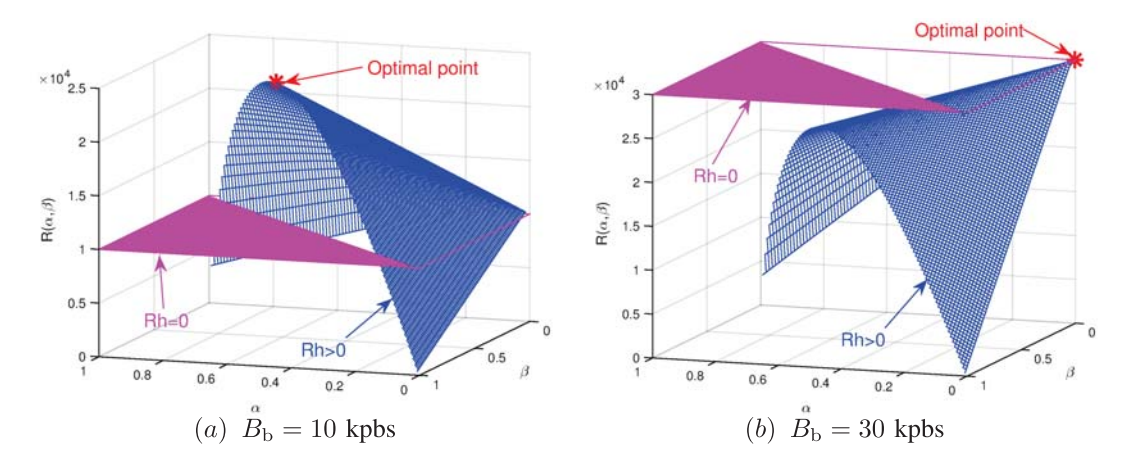


Fig. 9. The overall transmission rate $R(\alpha, \beta)$ under different value of B_b .

policies, namely, the backscatter only policy (BP) and harvestthen-transmit only policy (HP). With the proposed solution, the overall transmission rate is approximately 2 times greater than that of the HP and 1.3 times greater than that of the BP when the channel idle periods are 0.1 and 0.6, respectively. Here, for the HP policy, its transmission rate first increases when the value of β increases from 0.1 to 0.3, but if the value of β keeps increasing, its transmission rate will be reduced. The reason is that when the channel idle period is small, the ST will have less time to transmit data. On the contrary, if the channel idle period is large, the ST will have less time for harvesting energy.

Next, we vary the backscatter transmission rate and evaluate the optimal solution together with the performance of the secondary system. Note that the backscatter transmission rate depends on the hardware configuration of the wireless node as stated in [6]. Here, we set the channel idle period at 0.3. In particular, as shown in Fig. 8(a), as the backscatter transmission rate is increased from 1 kbps to 21 kbps, the ST will always choose the harvest-then-transmit mode, i.e., $\alpha = 1$. However, if the backscatter transmission rate keeps increasing, the ST will spend more time for the backscatter mode. When it is greater than 45 kbps, the ST will use the backscatter mode only. Again, here the proposed solution always achieves the best performance compared with those of the BP and the HP as shown in Fig. 8(b).

Then, we examine the transmission policy of the ST under different wireless signals from selected practical RF sources. Specifically, in Fig. 8(c), we study three different signals, i.e., FM signals, TV signals, and WiFi signals. As observed in

Fig. 8(c), the ST will only select the harvest-then-transmit mode when the backscatter transmission rate is lower than 17 kbps and 1 kbps for TV signals and WiFi signals, respectively. This can be explained through the Friis equation in (3). In particular, for TV signals and WiFi signals, because they are transmitted at high frequencies (i.e., 915 MHz and 2.4 GHz, respectively), the amount of energy harvested at the ST will be reduced significantly as compared with the FM signal (100 MHz). For WiFi signals, although the secondary system can be placed near the power source, e.g., an access point, the source's transmit power is relatively small (around 10 dBm as shown in Table I) and the frequency is very high (few GHz). Therefore, the amount of harvested energy is very small. Consequently, the ST tends to spend more time for the backscatter mode.

C. Underlay Cognitive Radio Networks

In this section, we first examine the objective function, i.e., the overall transmission rate, under the variation of the values of α and β , i.e., $R(\alpha, \beta)$ in (28). In Figs. 9(a) and (b), we consider two cases, i.e., $B_b = 10$ kbps and 30 kbps, respectively. For $B_b = 10$ kbps, the optimal values of α and β are 0.682 and 0.318, respectively. This corresponds to the case when $\tau = \alpha + \beta = 1$, i.e., the ST will select the harvest-then-transmit mode. Conversely, for $B_b = 30$ kbps (Fig. 9(b)), the optimal solution is at $\alpha = 0$ and $\beta = 0$ (corresponding to $\tau = 0$). This implies that the ST will use the backscatter mode in this case. This result also confirms the findings in Section IV, i.e., the optimal transmission policy of the ST is a step function.

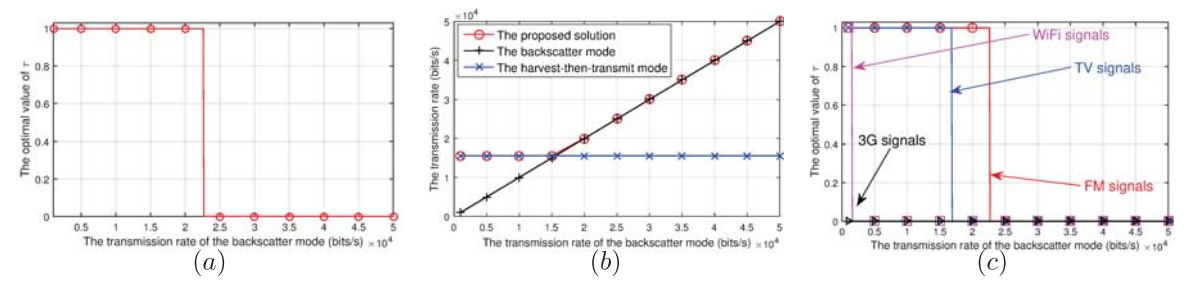


Fig. 10. The performance of the system under the variation of transmission bit rate of the backscatter mode.

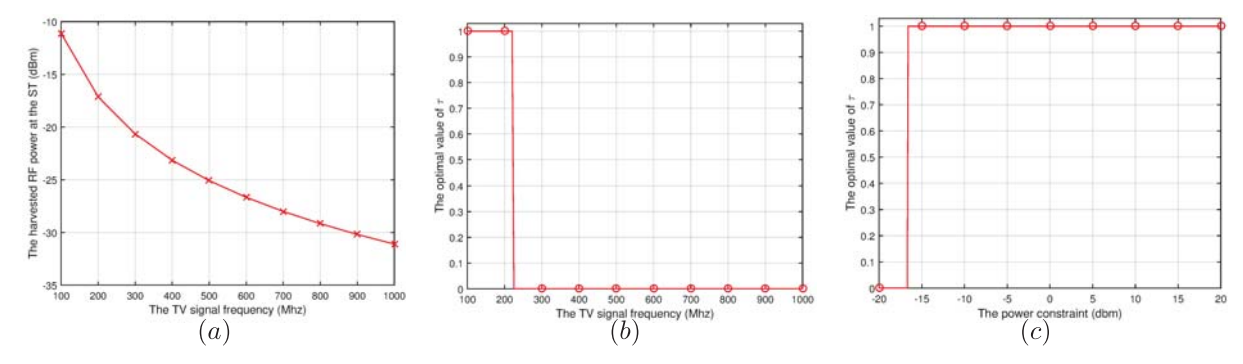


Fig. 11. The harvested RF power (a) and the optimal policy (b) of the ST when the TV signal frequency is varied, and the optimal policy of the ST (c) under the variation of the power constraint P^{\ddagger} .

We also vary the transmission rate of the backscatter mode and evaluate the policy along with the performance of the secondary system. As observed in Fig. 10 (a), as the backscatter transmission rate increases, the optimal value of τ will be reduced. Here, note that as stated in Section IV, the variation of τ is a step function. In particular, in Fig. 10(a), the ST will select the harvest-then-transmit mode if the backscatter transmission rate is lower than 22.6 kpbs, and the backscatter mode otherwise. Again, as shown in Fig. 10(b), it is confirmed that the proposed solution always achieves the best performance in terms of the overall transmission rate for the secondary system.

In Fig. 10(c), similar to the overlay CRNs, we also compare the proposed solution of the ST under different types of wireless signals. We examine four different types of signals, i.e., FM signals, TV signals, WiFi signals, and 3G mobile signals, which are generally considered in underlay CRNs. Similar to the overlay CRN, the decision of the ST also depends on the characteristic of the received signal. For WiFi and 3G signals, although the secondary system can be placed near the power source, e.g., an access point and cellular base station, the source's transmit power is relatively small (around 10 dBm as shown in Table I) and the frequency is very high (few GHz). Therefore, the amount of harvested energy is very small, and thus the ST will prefer using the backscatter mode in the cases of WiFi and 3G signals.

We vary the signal frequency (Fig. 11 (a) and (b)) and the transmit power constraint (Fig. 11 (c)) of the secondary system to investigate their impacts to the optimal policy of the ST. In particular, it is observed that as the frequency of the signal increases, the amount of harvested energy will be reduced (Fig. 11(a)), and hence the backscatter mode will be more preferable (Fig. 11(b)). In Fig. 11 (c), we observe that when the transmit power constraint of the secondary system is more

relaxed (i.e., the power threshold increases), the optimal value of τ also increases. This implies that the ST tends to choose the harvest-then-transmit mode. The reason is that when the transmit power constraint is limited at a low level, the ST cannot fully utilize the harvested energy. Consequently, the ST will use the backscatter mode instead.

Through simulation results and analysis presented in the previous sections, we can draw the following conclusions which are especially useful in implementing optimal techniques for sensors in practice.

- For the primary channel operating in the overlay configuration, the channel idle period is one of the most important factors which impacts to the optimal time tradeoff problem of the sensor. If the channel is almost idle, the sensor should use the harvest-then-transmit mode, while if the channel is almost busy, the sensor should perform backscatter mode.
- For the primary channel operating in the underlay configuration, we just need to implement either harvest-then-transmit or backscatter mode on the sensor. In particular, we can simply compare the threshold of the backscatter mode B_b^* , found in Section IV, with the sensor's backscatter rate and then choose the optimal mode for the sensor.
- For the primary signal with very low transmit power and very high frequency, e.g., 3G and WiFi signals, the amount of energy harvested is often very low, and thus the sensor usually adopts the backscatter mode to maximize its throughput.

VI. CONCLUSIONS AND FUTURE WORK

In this paper, we have introduced a new concept of integrating ambient backscatter communication with RF-powered cognitive radio networks (CRNs). We have also investigated the performance of the secondary system in both overlay

and underlay CRNs. In both cases, we have formulated the optimization problems for the ST and solved them to obtain the optimal transmission policy. Through numerical results, we have demonstrated that by incorporating the ambient backscatter communication and the conventional harvest-then-transmit protocol in RF-powered CRNs, the secondary system always achieves the best performance under any setups. Moreover, the numerical results in this paper can provide insightful guidance for the wireless nodes to choose the best mode to operate. For the future work, we will extend the system model with multiple secondary users coexisting in the same environment, and we will also consider the case with dual band ambient energy harvesting.

APPENDIX A THE PROOF OF THEOREM 1

Proof: Since $\alpha^{\dagger} \leq 1$ and $\alpha^{\dagger} \leq \alpha$, then from (10), we

$$R_{\rm h} = \mu \kappa W \log_2 \left[1 + \frac{1}{P_0 \mu} (\alpha (1 - \beta) P_{\rm R} - E_{\rm c}) \right].$$
 (46)

To prove Theorem 1, we denote $a = \kappa W$, $b = \frac{1}{P_0} (\alpha(1 - \alpha)^2)$ β) $P_{\rm R} - E_{\rm c}$), where a and b are positive constants since now we consider R_h as a function of μ . Then, (10) becomes

$$R_{\rm h}(\mu) = a\mu \log_2\left(1 + \frac{b}{\mu}\right). \tag{47}$$

We then derive the first and second derivatives of R_h with respect to μ as follows:

$$R'_{h}(\mu) = a \log_{2} \left(1 + \frac{b}{\mu} \right) - \frac{ab}{(\mu + b) \ln 2}, \tag{48}$$

$$R''_{h}(\mu) = -\frac{ab^{2}}{\mu(\mu + b)^{2} \ln 2}. \tag{49}$$

$$R_h''(\mu) = -\frac{ab^2}{\mu(\mu+b)^2 \ln 2}. (49)$$

From (49), we observe that $R_h^{''} < 0$ since a, b, and μ are greater than 0. Hence, $R'_h(\mu)$ is a decreasing function of μ . Moreover, from (48), we derive the following result

$$\lim_{\mu \to +\infty} R_h'(\mu) = \lim_{\mu \to +\infty} a \log_2 \left(1 + \frac{b}{\mu} \right) - \lim_{\mu \to +\infty} \frac{ab}{(\mu + b) \ln 2}$$

$$= 0. \tag{50}$$

When $\mu \to +\infty$, $R'_h(\mu) = 0$, this implies that $R'_h(\mu) >$ $0, \forall \mu \in [0, \beta]$. As a result, $R_h(\mu)$ is an increasing function over $\mu \in [0, \beta]$, and thus $\max_{\mu} R_h(\mu) = R_h(\beta), \forall \mu \in [0, \beta]$. The proof is now completed.

APPENDIX B The Proof of Theorem 2

Proof: For $\alpha \in [\alpha^{\dagger}, 1]$ and $\alpha^{\dagger} < 1$, from (14) we obtain the first and second derivatives of $R(\alpha)$ with respect to α as follows:

$$R'(\alpha) = -B_b(1-\beta) + \frac{\beta \kappa W m}{(m\alpha + n) \ln 2},\tag{51}$$

$$R''(\alpha) = -\frac{\beta \kappa W m^2}{(m\alpha + n)^2 \ln 2} < 0, \ \forall \alpha.$$
 (52)

From (52), we can infer that $R'(\alpha)$ is a decreasing function of α . Furthermore, to guarantee that there exists a value of $\alpha \in$

 $[\alpha^{\dagger}, 1]$ such that $R'(\alpha) = 0$, we have the following boundary conditions

$$R'(\alpha^{\dagger}) = -B_{b}(1-\beta) + \frac{\beta \kappa Wm}{(m\alpha^{\dagger} + n) \ln 2} > 0,$$

and

$$R'(1) = -B_b(1-\beta) + \frac{\beta \kappa W m}{(m+n) \ln 2} < 0.$$
 (53)

Then, from (53), we have the following condition

$$B_{\rm b} \in \left(\frac{\beta \kappa W m}{(m+n)(1-\beta)\ln 2}, \frac{\beta \kappa W m}{(m\alpha^{\dagger}+n)(1-\beta)\ln 2}\right).$$
 (54)

Here, let $\alpha^* \in [\alpha^{\dagger}, 1]$ be an optimal point of the objective function $R(\alpha)$. From (51), we have

$$\alpha^* = \frac{\beta \kappa W}{B_{\rm b}(1-\beta)\ln 2} - \frac{n}{m}.\tag{55}$$

Then, we can conclude that if the condition in (54) is met, we can always find an optimal solution $\alpha^* \in [\alpha^{\dagger}, 1]$ such that $R'(\alpha^*) = 0.$

From (52), we show that $R(\alpha)$ is a concave function. This implies that the optimal solution α^* is globally optimal, and

 $B_b \in \left(\frac{\beta \kappa W m}{(m+n)(1-\beta) \ln 2}, \frac{\beta \kappa W m}{(m\alpha^\dagger + n)(1-\beta) \ln 2}\right)$, then we can always find a globally optimal solution $\alpha^* = \frac{\beta \kappa W}{B_b(1-\lambda) \ln 2} - \frac{n}{m}$ which maximizes the objective function R.

APPENDIX C

THE PROOF OF THEOREM 3

Proof: First, we will prove that if $B_b \ge \frac{\beta \kappa W m}{(m\alpha^{\dagger} + n)(1-\beta) \ln 2}$, then $\alpha^* = \alpha^{\dagger}$. Since $B_b \geq \frac{\beta \kappa W m}{(m\alpha^{\dagger} + n)(1-\beta) \ln 2}$, from (51), we have the following result

$$R'(\alpha) \leq -\frac{\beta \kappa W m}{(m\alpha^{\dagger} + n) \ln 2} + \frac{\beta \kappa W m}{(n + m\alpha) \ln 2}$$
$$\leq \frac{\beta \kappa W m^{2} (\alpha^{\dagger} - \alpha)}{(n + m\alpha)(m\alpha^{\dagger} + n) \ln 2} \leq 0, \quad \forall \alpha \in [\alpha^{\dagger}, 1]. \quad (56)$$

From (56), there are two cases, i.e., $R'(\alpha) = 0$ or $R'(\alpha) < 0$. If $R'(\alpha) = 0$, i.e., $\alpha = \alpha^{\dagger}$, then $\alpha^* = \alpha^{\dagger}$. If $R'(\alpha) < 0$, then $R(\alpha)$ is a decreasing function of α . Therefore, $R_{\text{max}}(\alpha) =$ $R(\alpha^{\dagger})$. It means that $\alpha^* = \alpha^{\dagger}$.

Second, we will prove that for $B_b \leq \frac{\beta \kappa Wm}{(m+n)(1-\beta)\ln 2}$, the ST will always select the harvest-then-transmit mode to maximize the objective function R. Since $B_b \leq \frac{\beta \kappa Wm}{(m+n)(1-\beta)\ln 2}$, from (51), we have the following result

$$R'(\alpha) \ge -\frac{\beta \kappa W m}{(m+n)\ln 2} + \frac{\beta \kappa W m}{(n+m\alpha)\ln 2}$$
$$\ge \frac{\beta \kappa W m^2 (1-\alpha)}{(m+n)(n+m\alpha)\ln 2}.$$
 (57)

Since $(n + m\alpha) > 0$ and m > 0 (from (10)), we have $(n + m) > (n + m\alpha) > 0, \forall \alpha \in [\alpha^{\dagger}, 1].$ Consequently, $R'(\alpha) \geq 0, \forall \alpha \in [\alpha^{\dagger}, 1]$. Here, we have two cases, i.e., $R'(\alpha) =$ 0 or $R'(\alpha) > 0$. If $R'(\alpha) = 0$, i.e., $\alpha = 1$, then $\alpha^* = 1$. If $R'(\alpha) > 0$, then $R(\alpha)$ is an increasing function of α . Therefore, for $\alpha^* = 1$, the ST will always choose the harvest-then-transmit

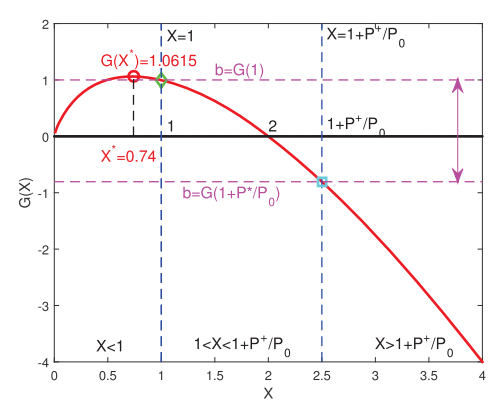


Fig. 12. Function G(X).

mode to maximize its overall transmission rate when $B_b \le \frac{\beta \kappa Wm}{(m+n)(1-\beta) \ln 2}$.

The proof is now completed.

APPENDIX D THE PROOF OF THEOREM 4

Proof: We first define $X=b+\frac{c}{\gamma}$. Then, we will prove that X>1 and $X\leq 1+\frac{P^{\ddagger}}{P_0}$ if γ satisfies \mathbb{C}_2 . From the first constraint in \mathbb{C}_2 , we have $\gamma<\frac{P_{\mathbb{R}}}{P_{\mathbb{C}}+P_{\mathbb{R}}}$, so

$$X = b + \frac{c}{\gamma} > b + \frac{c}{\frac{P_{R}}{P_{c} + P_{R}}} \text{ (since } c, \gamma > 0),$$

$$> 1 - \frac{P_{R} + P_{c}}{P_{0}} + \frac{\frac{P_{R}}{P_{0}}}{\frac{P_{R}}{P_{0} + P_{D}}} = 1 \text{ (from (36))}.$$
(58)

From the second constraint in C_2 , we have $\gamma \geq \frac{P_R}{P_c + P^{\ddagger} + P_R}$, so

$$X = b + \frac{c}{\gamma} \le b + \frac{c}{\frac{P_{R}}{P_{c} + P^{\ddagger} + P_{R}}} \text{ (since } c, \gamma > 0),$$

$$\le 1 - \frac{P_{R} + P_{c}}{P_{0}} + \frac{\frac{P_{R}}{P_{0}}}{\frac{P_{R}}{P_{0} + P^{\ddagger} + P_{0}}} = 1 + \frac{P^{\ddagger}}{P_{0}} \text{ (from (36))}. (59)$$

From (38), we have

$$g(X) = R'_h = a \log_2(b + \frac{c}{\gamma}) - \frac{ac}{(b\gamma + c)\ln 2},$$

$$= \frac{a}{\ln 2} \left(\ln(b + \frac{c}{\gamma}) + \frac{b}{b + \frac{c}{\gamma}} - 1 \right),$$

$$= \frac{a}{\ln 2} \left(\ln X + \frac{b}{X} - 1 \right),$$

$$= \frac{a}{X \ln 2} \left(X \ln X + b - X \right). \tag{60}$$

Then, we need to find the value of $X \in (1, 1 + \frac{p^{\ddagger}}{P_0}]$ that satisfies $g(X) = R'_h(\gamma) = 0$. It means

$$\frac{a}{X\ln 2} \left(X\ln X + b - X \right) = 0,$$

$$X - X\ln X = b \text{ (since } a > 0 \text{ and } X > 1). \tag{61}$$

We denote $G(X) = X - X \ln X$. Then from Fig. 12, we can conclude that if $b \in [G(1 + \frac{P^{\ddagger}}{P_0}), G(1)]$, then we can always find a unique solution X^* satisfying the condition in (60).

Since $X = b + \frac{c}{\gamma}$, we can conclude that if $b \in [G(1 + \frac{P^{\ddagger}}{P_0}), G(1)]$, then we can always find a unique solution $\gamma_1^* =$

 $\frac{c}{X^*-b}$ which satisfies $R_h'(\gamma_1^*)=0.$ Moreover, we have $b=1-\frac{P_{\rm R}+P_{\rm c}}{P_0}$, so we always have b< G(1)=1. Therefore, if $b=1-\frac{P_{\rm R}+P_{\rm c}}{P_0}\geq G(1+\frac{P^{\ddagger}}{P_0})=(1+\frac{P^{\ddagger}}{P_0})(1-\ln(1+\frac{P^{\ddagger}}{P_0})),$ then we can always find a unique solution γ_1^* such that $R_h'(\gamma_1^*)=0.$

Moreover, from (38), we can derive the second derivative of R_h as follows:

$$R_h^{"} = -\frac{ac^2}{(b\gamma + c)^2 \gamma \ln 2}. (62)$$

Here, since $a = \kappa W > 0$, $\gamma > 0$, and c > 0, $R''_h < 0$. This means that R_h is a concave function. Therefore, if γ_1^* is an optimal solution of \mathbf{P}_2 , then it is a unique globally optimal solution, and γ_1^* maximizes the objective function R_h .

The proof is now completed.

APPENDIX E THE PROOF OF THEOREM 5

Proof: From (60), we have $R_h'(\gamma) = g(X) = \frac{a}{X \ln 2}(b-G(X))$. Since $X \in (1, 1+\frac{P^{\ddagger}}{P_0}]$ (as shown in Fig. 12), if $b < G(1+\frac{P^{\ddagger}}{P_R})$, i.e., $1-\frac{P_R+P_c}{P_0} < (1+\frac{P^{\ddagger}}{P_0})\left(1-\ln(1+\frac{P^{\ddagger}}{P_0})\right)$, then $R_h'(\gamma) = g(X) < 0$. This implies that R_h is a decreasing function of γ . Thus, there exists a unique solution of γ_2^* such that $R_h(\gamma_2^*)$ is maximized. Additionally, from C_2 , we have $\gamma \in [\frac{P_R}{P_c+P^{\ddagger}+P_R},\frac{P_R}{P_c+P_R})$. Thus, $\gamma_2^* = \frac{P_R}{P_c+P^{\ddagger}+P_R}$. The proof is now completed.

REFERENCES

- [1] D. T. Hoang, D. Niyato, P. Wang, D. I. Kim, and Z. Han, "The tradeoff analysis in RF-powered backscatter cognitive radio networks," in *Proc. IEEE Global Commun. Conf.*, Washington, DC, USA, Feb. 2017, pp. 1–6.
- [2] S. Lee, R. Zhang, and K. Huang, "Opportunistic wireless energy harvesting in cognitive radio networks," *IEEE Trans. Wireless Commun.*, vol. 12, no. 9, pp. 4788–4799, Sep. 2013.
- [3] S. Lee and R. Zhang, "Cognitive wireless powered: Spectrum sharing models and throughput maximization," *IEEE Trans. Cognit. Commun. Netw.*, vol. 1, no. 3, pp. 335–346, Sep. 2015.
- [4] S. Bi, Y. Zeng, and R. Zhang, "Wireless powered communication networks: An overview," *IEEE Wireless Commun.*, vol. 23, no. 4, pp. 10–18, Apr. 2016.
- [5] H. Ju and R. Zhang, "Throughput maximization in wireless powered communication networks," *IEEE Trans. Wireless Commun.*, vol. 13, no. 1, pp. 418–428, Jan. 2014.
- [6] V. Liu, A. Parks, V. Talla, S. Gollakota, D. Wetherall, and J. R. Smith, "Ambient backscatter: Wireless communication out of thin air," in *Proc. ACM SIGCOMM*, Hong Kong, China, Aug. 2013, pp. 39–50.
- [7] A. N. Parks, A. Liu, S. Gollakota, and J. S. Smith, "Turbocharging ambient backscatter communication," ACM SIGCOMM Comput. Commun. Rev., vol. 44, no. 4, pp. 619–630, Oct. 2014.
- [8] B. Kellogg, A. Parks, S. Gollakota, J. R. Smith, and D. Wetherall, "Wi-Fi backscatter: Internet connectivity for RF-powered devices," in Proc. ACM SIGCOMM, Chicago, IL, USA, Aug. 2014, pp. 607–618.
- [9] P. Zhang and D. Ganesan, "Enabling bit-by-bit backscatter communication in severe energy harvesting environments," in *Proc. 11th USENIX Conf. Netw. Syst. Design Implement.*, Seattle, WA, USA, Apr. 2014, pp. 345–357.
- [10] D. T. Hoang, D. Niyato, P. Wang, and D. I. Kim, "Performance optimization for cooperative multiuser cognitive radio networks with RF energy harvesting capability," *IEEE Trans. Wireless Commun.*, vol. 14, no. 7, pp. 3614–3629, Jul. 2015.
- [11] S. Park, H. Kim, and D. Hong, "Cognitive radio networks with energy harvesting," *IEEE Trans. Wireless Commun.*, vol. 12, no. 3, pp. 1386–1397, Mar. 2013.
- [12] S. A. Mousavifar, Y. Liu, C. Leung, M. Elkashlan, and T. Q. Duong, "Wireless energy harvesting and spectrum sharing in cognitive radio," in *Proc. IEEE 80th Veh. Technol. Conf. (VTC Fall)*, Sep. 2014, pp. 1–5.

- [13] D. T. Hoang, D. Niyato, P. Wang, and D. I. Kim, "Opportunistic channel access and RF energy harvesting in cognitive radio networks," *IEEE J. Sel. Areas Commun.*, vol. 32, no. 11, pp. 2039–2052, Nov. 2014.
- [14] Z. Wang, Z. Chen, Y. Yao, B. Xia, and H. Liu, "Wireless energy harvesting and information transfer in cognitive two-way relay networks," in *Proc. IEEE Global Commun. Conf. (GLOBECOM)*, Dec. 2014, pp. 3465–3470.
 [15] V. Rakovic, D. Denkovski, Z. Hadzi-Velkov, and L. Gavrilovska,
- [15] V. Rakovic, D. Denkovski, Z. Hadzi-Velkov, and L. Gavrilovska, "Optimal time sharing in underlay cognitive radio systems with RF energy harvesting," in *Proc. IEEE Int. Conf. Commun.*, London, U.K., Jun. 2015, pp. 7689–7694.
- [16] S. Yin, E. Zhang, Z. Qu, L. Yin, and S. Li, "Optimal cooperation strategy in cognitive radio systems with energy harvesting," *IEEE Trans. Wireless Commun.*, vol. 13, no. 9, pp. 4693–4707, Sep. 2014.
- [17] 'Ambient Backscatter' Brings Us Closer to an Internet of Things, accessed on Jun. 6, 2017. [Online]. Available: https://www.fastcodesign.com/3017570/ambient
- [18] C. Pérez-Penichet, A. Varshney, F. Hermans, C. Rohner, and T. Voigt, "Do multiple bits per symbol increase the throughput of ambient backscatter communications?" in *Proc. Int. Conf. Embedded Wireless* Syst. Netw., TU Graz, Austria, Feb. 2016, pp. 355–360.
- [19] J. You, G. Wang, and Z. Zhong, "Physical layer security-enhancing transmission protocol against eavesdropping for ambient backscatter communication system," in *Proc. 6th Int. Conf. Wireless, Mobile Multi-Media*, Beijing, China, Feb. 2015, pp. 43–47.
- [20] K. Lu, G. Wang, F. Qu, and Z. Zhong, "Signal detection and BER analysis for RF-powered devices utilizing ambient backscatter," in *Proc. Int. Conf. Wireless Commun. Signal Process.*, Nanjing, China, Oct. 2015, pp. 1–5.
- [21] RFD102A: Wireless Energy Harvesting Module, accessed on Jun. 6, 2017. [Online]. Available: http://www.rfdiagnostics.com/ product/rfd102a/
- [22] ADG902 RF Switch Datasheet, accessed on Jun. 6, 2017.
 [Online]. Available: http://www.analog.com/static/imported-files/data_sheets/adg901_902.pdf
- [23] Singapore Disney Channel Schedule, accessed on Jun. 6, 2017. [Online]. Available: http://disneychannel.disney.sg/tv-schedule
- [24] D. Darsena, G. Gelli, and F. Verde, "Modeling and performance analysis of wireless networks with ambient backscatter devices," *IEEE Trans. Commun.*, vol. 65, no. 4, pp. 1797–1814, Jan. 2017.
- [25] G. Wang, F. Gao, R. Fan, and C. Tellambura, "Ambient backscatter communication systems: Detection and performance analysis," *IEEE Trans. Commun.*, vol. 64, no. 11, pp. 4836–4846, Nov. 2016.
- [26] J. Qian, F. Gao, and G. Wang, "Signal detection of ambient backscatter system with differential modulation," in *Proc. IEEE Int. Conf. Acoust.*, Speech Signal Process., Mar. 2016, pp. 3831–3835.
- [27] R. H. Walden, "Analog-to-digital converter survey and analysis," *IEEE J. Sel. Areas Commun.*, vol. 17, no. 4, pp. 539–550, Apr. 1999.
- [28] C. A. Balanis, Antenna Theory: Analysis and Design. New York, NY, USA: Wiley, 2012.
- [29] H. Huang and V. K. N. Lau, "Decentralized delay optimal control for interference networks with limited renewable energy storage," *IEEE Trans. Signal Process.*, vol. 60, no. 5, pp. 2552–2561, May 2012.
- [30] G. Zheng, Z. Ho, E. A. Jorswieck, and B. Ottersten, "Information and energy cooperation in cognitive radio networks," *IEEE Trans. Signal Process.*, vol. 62, no. 9, pp. 2290–2303, May 2014.
- [31] B. Cho, K. Koufos, and R. Jantti, "Interference control in cognitive wireless networks by tuning the carrier sensing threshold," in *Proc. IEEE Int. Conf. Cognit. Radio Oriented Wireless Netw.*, Washington, DC, USA, Jul. 2013, pp. 282–287.
- [32] D. Y. Kim and D. I. Kim, "Reverse-link interrogation range of a UHF MIMO-RFID system in Nakagami-m fading channels," *IEEE Trans. Ind. Electron.*, vol. 57, no. 4, pp. 1468–1477, Apr. 2010.



Dinh Thai Hoang (M'16) received the Ph.D. degree in from the School of Computer Science and Engineering, Nanyang Technological University, Singapore, 2016, where he is currently a Research Fellow. His research interests include optimization problems and game theory for wireless communication networks and mobile cloud computing.



Dusit Niyato (M'09–SM'15–F'17) received the B.Eng. degree from King Mongkut's Institute of Technology Ladkrabang, Thailand, in 1999, and the Ph.D. degree in electrical and computer engineering from the University of Manitoba, Canada, in 2008. He is currently an Associate Professor with the School of Computer Science and Engineering, Nanyang Technological University, Singapore. His research interests are in the area of energy harvesting for wireless communication, Internet of Things, and sensor networks.



Ping Wang (M'08–SM'15) received the Ph.D. degree in electrical engineering from the University of Waterloo, Canada, in 2008. She is currently an Associate Professor with the School of Computer Science and Engineering, Nanyang Technological University, Singapore. Her current research interests include resource allocation in multimedia wireless networks, cloud computing, and smart grid. She was a co-recipient of the Best Paper Award from the IEEE Wireless Communications and Networking Conference in 2012 and the IEEE International

Conference on Communications in 2007.



Dong In Kim (S'89–M'91–SM'02) received the Ph.D. degree in electrical engineering from the University of Southern California, Los Angeles, CA, USA, in 1990. He was a Tenured Professor with the School of Engineering Science, Simon Fraser University, Burnaby, BC, Canada. Since 2007, he has been with Sungkyunkwan University, Suwon, South Korea, where he is currently a Professor with the College of Information and Communication Engineering. He is a first recipient of the NRF of Korea Engineering Research Center in Wireless

Communications for RF Energy Harvesting from 2014 to 2021. From 2002 to 2011, he served as an Editor and Founding Area Editor of Cross-Layer Design and Optimization for the IEEE TRANSACTIONS ON WIRELESS COMMUNICATIONS. From 2008 to 2011, he served as the Co-Editor-in-Chief of the IEEE/KICS JOURNAL OF COMMUNICATIONS AND NETWORKS. He served as the Founding Editor-in-Chief of the IEEE WIRELESS COMMUNICATIONS LETTERS from 2012 to 2015. From 2001 to 2014, he served as an Editor of Spread Spectrum Transmission and Access for the IEEE TRANSACTIONS ON COMMUNICATIONS. He is currently serving as an Editor-at-Large of Wireless Communication I for the IEEE TRANSACTIONS ON COMMUNICATIONS.



Zhu Han (S'01–M'04–SM'09–F'14) received the B.S. degree in electronic engineering from Tsinghua University, in 1997, and the M.S. and Ph.D. degrees in electrical and computer engineering from the University of Maryland, College Park, in 1999 and 2003, respectively. From 2000 to 2002, he was a Research and Development Engineer of JDSU, Germantown, MD, USA. From 2003 to 2006, he was a Research Associate with the University of Maryland. From 2006 to 2008, he was an Assistant Professor with Boise State University, Idaho. He is

currently a Professor with the Electrical and Computer Engineering Department and the Computer Science Department, University of Houston, Texas. His research interests include wireless resource allocation and management, wireless communications and networking, game theory, big data analysis, security, and smart grid. He received an NSF Career Award in 2010, the Fred W. Ellersick Prize of the IEEE Communication Society in 2011, the EURASIP Best Paper Award for the *Journal on Advances in Signal Processing* in 2015, IEEE Leonard G. Abraham Prize in the field of Communications Systems (Best Paper Award in IEEE JSAC) in 2016, and several best paper awards in IEEE conferences. He is also an IEEE Communications Society Distinguished Lecturer.